Journal of Southeast University (English Edition) Vol. 29, No. 4, pp. 384 – 388 Dec. 2013 ISSN 1003—7985

Two-level Bregmanized method for image interpolation with graph regularized sparse coding

Liu Qiegen[1,2] Zhang Minghui[1] Liang Dong[2]

([1]Department of Electronic Information Engineering, Nanchang University, Nanchang 330031, China)
([2]Paul C. Lauterbur Research Centre for Biomedical Imaging, Shenzhen Institutes of Advanced Technology, Chinese Academy of Sciences, Shenzhen 518055, China)

Abstract: A two-level Bregmanized method with graph regularized sparse coding (TBGSC) is presented for image interpolation. The outer-level Bregman iterative procedure enforces the observation data constraints, while the inner-level Bregmanized method devotes to dictionary updating and sparse represention of small overlapping image patches. The introduced constraint of graph regularized sparse coding can capture local image features effectively, and consequently enables accurate reconstruction from highly undersampled partial data. Furthermore, modified sparse coding and simple dictionary updating applied in the inner minimization make the proposed algorithm converge within a relatively small number of iterations. Experimental results demonstrate that the proposed algorithm can effectively reconstruct images and it outperforms the current state-of-the-art approaches in terms of visual comparisons and quantitative measures.

Key words: image interpolation; Bregman iterative method; graph regularized sparse coding; alternating direction method
doi: 10.3969/j. issn. 1003 – 7985. 2013. 04. 006

Image interpolation is a fundamental and widely studied problem in image processing. It aims to recover a plausible image from incomplete data (e. g., pixels sampled at a subset region). Since this problem is ill-posed, incorporating some prior knowledge into the recovery is needed. The conventional image interpolation algorithms mostly exploit the local correlation of image pixels. For example, B-spline interpolation[1] employed cubic splines to fit the local intensity/regression function; and the kernel regression (KR) framework used adaptive local covariance structures to locally guide the linear or higher order regression for interpolation[2]. Zhang et al.[3] presented a local coherent autoregressive (AR) model, which assumed that the underlying image is piecewise stationary. Motivated by recent progress in local intrinsic manifold assumption, Liu et al.[4] developed a graph-Laplacian regularized local linear regression method (RLLR), which used the geometric structure of the marginal probability distribution as an additional local smoothness-preserving constraint.

Some algorithms based on nonlocal and similarity priors have attracted much attention in the past few years. For instance, the success of the patch-based nonlocal method (PN) depends on iteratively projecting onto two convex sets: one is given by the observation data and the other is defined by the sparsity-based nonlocal prior BM3D[5]. Dong et al.[6] combined the promising sparse representation and nonlocal auto-regression model for interpolation.

More recently, the combinations of local and nonlocal priors have received an increasing amount of interest. Zheng et al.[7] presented a graph regularized sparse coding (GraphSC) algorithm, which introduces a k-nearest neighbor graph into the sparse coding objective function as a regularizer for image classification. In this paper, we propose a two-level Bregmanized method with graph regularized sparse coding (TBGSC). The GraphSC prior is incorporated into a two-level Bregmanized iterative procedure to achieve better recovery ability and computation efficiency for image interpolation.

1 Preliminary

1.1 Bregman iterative method and augmented Lagrangian scheme

The augmented Lagrangian (AL) method is a promising technique and used in various image recovery problems[8-9]. Consider the following optimization problem with linear equality constraint:

$$\min E(\boldsymbol{\alpha}) \qquad \text{s. t. } \boldsymbol{A\alpha} = \tilde{\boldsymbol{I}} \tag{1}$$

It can be solved by the standard AL method; i. e. the solution of Eq. (1) is achieved by solving a sequence of unconstrained subproblems, in which the objective function is formed by adding the additional "penalty" terms to the objective function of the original constrained optimization. The "penalty" terms are made up of constrained functions multiplied by a positive coeffi-

Received 2013-07-21.
Biography: Liu Qiegen (1983—), male, doctor, lecturer, liuqiegen@ncu. edu. cn.
Foundation items: The National Natural Science Foundation of China (No. 61362001, 61102043, 61262084, 20132BAB211030, 20122BAB211015), the Basic Research Program of Shenzhen (No. JC201104220219A).
Citation: Liu Qiegen, Zhang Minghui, Liang Dong. Two-level Bregmanized method for image interpolation with graph regularized sparse coding[J]. Journal of Southeast University (English Edition), 2013, 29 (4): 384 – 388. [doi: 10.3969/j. issn. 1003 – 7985. 2013. 04. 006]

cient.

$$\left.\begin{aligned} \boldsymbol{\alpha}^{k+1} &= \arg\min E(\boldsymbol{\alpha}) + \langle \boldsymbol{y}_\mu^k, \tilde{\boldsymbol{I}} - \boldsymbol{A}\boldsymbol{\alpha}\rangle + \frac{\mu}{2}\|\tilde{\boldsymbol{I}} - \boldsymbol{A}\boldsymbol{\alpha}\|^2 \\ \boldsymbol{y}_\mu^{k+1} &= \boldsymbol{y}_\mu^k + \mu(\tilde{\boldsymbol{I}} - \boldsymbol{A}\boldsymbol{\alpha}^{k+1}) \end{aligned}\right\} \tag{2}$$

where $\boldsymbol{y}_\mu^k$ represents the vector of Lagrange multipliers and $\mu > 0$ is the penalty parameter. If we let $\boldsymbol{y} = \boldsymbol{y}_\mu/\mu$, then the iterative scheme (2) becomes the following alternative form:

$$\left.\begin{aligned} \boldsymbol{\alpha}^{k+1} &= \operatorname{argmin} E(\boldsymbol{\alpha}) + \frac{\mu}{2}\|\tilde{\boldsymbol{I}} + \boldsymbol{y}^k - \boldsymbol{A}\boldsymbol{\alpha}\|^2 \\ \boldsymbol{y}^k + \tilde{\boldsymbol{I}} &= \boldsymbol{y}^{k+1} + \boldsymbol{A}\boldsymbol{\alpha}^{k+1} \end{aligned}\right\} \tag{3}$$

Eq. (3) is often called the Bregman iterative method[10-11].

The relationship of the AL method and the Bregman iterative method was discussed in Ref. [10]. They are identical when the constraint is linear[8,11]. As explained in Refs. [10-11], the iterative procedure (3) has interesting multi-scale interpretation.

1.2 Graph regularized sparse coding

The effect of GraphSC lies on its manifold assumption. It states that if two data points $\boldsymbol{x}_i$, $\boldsymbol{x}_j$ are close in the intrinsic geometry of the data distribution, then their representations $\boldsymbol{s}_i$ and $\boldsymbol{s}_j$ in the new dictionary are also close to each other. Specially, a nearest neighbor graph G with M vertices is introduced, where each vertex represents a data point in $\boldsymbol{X}$, and $\boldsymbol{W}$ is the weight matrix of G. If $\boldsymbol{x}_i$ is among the k-nearest neighbors of $\boldsymbol{x}_j$, $W_{ij} = 1$; otherwise, $W_{ij} = 0$. Besides, the degree of $\boldsymbol{x}_i$ is defined as $d_i = \sum_{j=1}^{M} W_{ij}$ and $\boldsymbol{D} = \operatorname{diag}(d_1, d_2, \cdots, d_M)$, $\boldsymbol{L} = \boldsymbol{D} - \boldsymbol{W}$. Then a reasonable criterion for properly mapping the weighted graph G to sparse coefficients $\boldsymbol{S}$ is to minimize the following objective function[7]:

$$\frac{1}{2}\sum_{i=1}^{M}\sum_{j=1}^{M}(\boldsymbol{s}_i - \boldsymbol{s}_j)^2 W_{ij} = \operatorname{Tr}(\boldsymbol{S}\boldsymbol{L}\boldsymbol{S}^{\mathrm{T}}) \tag{4}$$

In short, the objective function of GraphSC consists of three terms: the empirical loss function, the Laplacian regularizer, and the L1-based sparse penalty function:

$$\begin{aligned} &\min_{\boldsymbol{B},\boldsymbol{S}} \frac{\lambda}{2}\|\boldsymbol{X} - \boldsymbol{B}\boldsymbol{S}\|_{\mathrm{F}}^2 + \alpha\operatorname{Tr}(\boldsymbol{S}\boldsymbol{L}\boldsymbol{S}^{\mathrm{T}}) + \sum_{i=1}^{M}\|\boldsymbol{s}_i\|_1 \\ &\text{s.t.} \quad \|\boldsymbol{b}_j\|^2 \leqslant 1 \quad \forall j = 1, 2, \cdots, J \end{aligned} \tag{5}$$

2 TBGSC Algorithm

In this section, the TBGSC algorithm for image interpolation is derived. We use $\boldsymbol{u}$ to represent the image to be reconstructed and $\boldsymbol{f}$ represents the observation data. These two variables are related as $\boldsymbol{F}_{\mathrm{p}}\boldsymbol{u} = \boldsymbol{f}$, where $\boldsymbol{F}_{\mathrm{p}}$ represents the partially sampled encoding matrix. Undersampling occurs when the number of samples is less than the number of image entries.

2.1 Outer-level Bregman iterative method

When considering the GraphSC as a regularizer, image recovery can be reformulated as follows:

$$\begin{aligned} &\min_{\boldsymbol{u}}\left\{\min_{\boldsymbol{B},\boldsymbol{S}} \frac{\lambda}{2}\|\boldsymbol{B}\boldsymbol{s}_i - \boldsymbol{R}_i\boldsymbol{u}\|_2^2 + \alpha\operatorname{Tr}(\boldsymbol{S}\boldsymbol{L}\boldsymbol{S}^{\mathrm{T}}) + \sum_i \|\boldsymbol{s}_i\|_1\right\} \\ &\text{s.t.} \quad \boldsymbol{F}_{\mathrm{p}}\boldsymbol{u} - \boldsymbol{f} = 0 \end{aligned} \tag{6}$$

By applying the Bregman iteration, the solution of Eq. (6) can be obtained by iteratively solving an unconstrained problem and then modifying the value of $\boldsymbol{f}$ used in the next iteration. It yields

$$\left.\begin{aligned} \boldsymbol{u}^{k+1} &= \arg\min_{\boldsymbol{u}}\left\{\min_{\boldsymbol{B},\boldsymbol{S}}\left(\alpha\operatorname{Tr}(\boldsymbol{S}\boldsymbol{L}\boldsymbol{S}^{\mathrm{T}}) + \sum_i\|\boldsymbol{s}_i\|_1 + \frac{\lambda}{2}\|\boldsymbol{B}\boldsymbol{s}_i - \boldsymbol{R}_i\boldsymbol{u}\|_2^2\right) + \frac{\mu}{2}\|\boldsymbol{F}_{\mathrm{p}}\boldsymbol{u} - \boldsymbol{f}^k\|_2^2\right\} \\ \boldsymbol{f}^{k+1} &= \boldsymbol{f}^k + \boldsymbol{f} - \boldsymbol{F}_{\mathrm{p}}\boldsymbol{u}^{k+1} \end{aligned}\right\} \tag{7}$$

A merit of the Bregman iteration is that the residual $\|\boldsymbol{F}_{\mathrm{p}}\boldsymbol{u}^{k+1} - \boldsymbol{f}\|_2$ of the sequence generated by Eq. (7) converges to zeros monotonically.

2.2 Inner-level Bregman iterative method

Denoting $\boldsymbol{X} = \boldsymbol{R}\boldsymbol{u}$ and employing operator splitting to the subproblem in Eq. (7), the unconstrained minimization problem is transformed to an equivalent constrained problem:

$$\begin{aligned} &\min_{\boldsymbol{B},\boldsymbol{S}} \frac{\lambda}{2}\|\boldsymbol{X} - \boldsymbol{Z}\|_{\mathrm{F}}^2 + \alpha\operatorname{Tr}(\boldsymbol{S}\boldsymbol{L}\boldsymbol{S}^{\mathrm{T}}) + \sum_{i=1}^{M}\|\boldsymbol{s}_i\|_1 \\ &\text{s.t.} \quad \boldsymbol{Z} = \boldsymbol{B}\boldsymbol{S} \\ &\qquad\ \|\boldsymbol{b}_j\|^2 \leqslant 1 \quad \forall j = 1, 2, \cdots, J \end{aligned} \tag{8}$$

The augmented Lagrangian function of problem (8) is

$$\begin{aligned} L(\boldsymbol{B},\boldsymbol{S},\boldsymbol{Z},\boldsymbol{Y}) = {}& \frac{\lambda}{2}\|\boldsymbol{X} - \boldsymbol{Z}\|_{\mathrm{F}}^2 + \alpha\operatorname{Tr}(\boldsymbol{S}\boldsymbol{L}\boldsymbol{S}^{\mathrm{T}}) + \\ & \sum_{i=1}^{M}\|\boldsymbol{s}_i\|_1 + \frac{\beta}{2}\left\|\boldsymbol{B}\boldsymbol{S} - \boldsymbol{Z} - \frac{\boldsymbol{Y}}{\beta}\right\|_{\mathrm{F}}^2 \end{aligned} \tag{9}$$

Since it is difficult to directly find the saddle point of the augmented Lagrangian function $L(\boldsymbol{B}, \boldsymbol{S}, \boldsymbol{Z}, \boldsymbol{Y})$, the alternating direction method is used to solve the following sub-problems individually and alternatively.

2.2.1 $\boldsymbol{S}$- and $\boldsymbol{Z}$-subproblems

First, the minimization of Eq. (9) with respect to $\boldsymbol{Z}$ can be analytically computed and $\boldsymbol{Z}$ can be eliminated. Specially, from the first and the forth terms of Eq. (9), we obtain the optimal solution:

$$\boldsymbol{Z} = \frac{\lambda\boldsymbol{X} + \beta(\boldsymbol{B}^k\boldsymbol{S} - \boldsymbol{Y}^k/\beta)}{\lambda + \beta} \tag{10}$$

Moreover, it follows that

$$\boldsymbol{Y}^{k+1}=\boldsymbol{Y}^{k}+\beta(-\boldsymbol{B}^{k}\boldsymbol{S}^{k+1}+\boldsymbol{Z}^{k+1})=\frac{\lambda\beta(\boldsymbol{X}-\boldsymbol{B}^{k}\boldsymbol{S}^{k+1}+\boldsymbol{Y}^{k}/\beta)}{\lambda+\beta} \tag{11}$$

Secondly, substituting $\boldsymbol{Z}$ of Eq. (10) into Eq. (9), it yields

$$\boldsymbol{S}^{k+1}=\arg\min_{S}\frac{\lambda\beta}{2(\lambda+\beta)}\left\|\boldsymbol{B}^{k}\boldsymbol{S}-\boldsymbol{X}-\frac{\boldsymbol{Y}^{k}}{\beta}\right\|_{\mathrm{F}}^{2}+\alpha\mathrm{Tr}(\boldsymbol{SLS}^{\mathrm{T}})+\sum_{i=1}^{M}\|\boldsymbol{s}_{i}\|_{1} \tag{12}$$

Note that when updating $\boldsymbol{s}_i$, the other vectors $\{\boldsymbol{s}_j\}_{j\neq i}$ are fixed. Thus, after some mathematical manipulation, we obtain the optimization problem for each $\boldsymbol{s}_i$:

$$\boldsymbol{s}_{i}^{k+1}=\arg\min_{s_i}\frac{\lambda\beta}{2(\lambda+\beta)}\left\|\boldsymbol{B}^{k}\boldsymbol{s}_{i}-\boldsymbol{x}_{i}-\frac{\boldsymbol{y}_{i}^{k}}{\beta}\right\|_{\mathrm{F}}^{2}+\alpha\boldsymbol{L}_{ii}\boldsymbol{s}_{i}^{\mathrm{T}}\boldsymbol{s}_{i}+\boldsymbol{s}_{i}^{\mathrm{T}}\boldsymbol{h}_{i}+\|\boldsymbol{s}_{i}\|_{1} \tag{13}$$

where $\boldsymbol{h}_i=2\alpha\sum_{j\neq i}\boldsymbol{L}_{ij}\boldsymbol{s}_j$.

Letting $g(\boldsymbol{s}_i)=\frac{\lambda\beta}{2(\lambda+\beta)}\left\|\boldsymbol{B}^{k}\boldsymbol{s}_{i}-\boldsymbol{x}_{i}-\frac{\boldsymbol{y}_{i}^{k}}{\beta}\right\|_{\mathrm{F}}^{2}+\alpha\boldsymbol{L}_{ii}\boldsymbol{s}_{i}^{\mathrm{T}}\boldsymbol{s}_{i}+\boldsymbol{s}_{i}^{\mathrm{T}}\boldsymbol{h}_{i}$, we have $\nabla g(\boldsymbol{s}_i)=\frac{\lambda\beta}{\lambda+\beta}(\boldsymbol{B}^{k})^{\mathrm{T}}\left(\boldsymbol{B}^{k}\boldsymbol{s}_{i}-\boldsymbol{x}_{i}-\frac{\boldsymbol{y}_{i}^{k}}{\beta}\right)+2\alpha\boldsymbol{L}_{ii}\boldsymbol{s}_{i}+\boldsymbol{h}_{i}$. Then following the iterative shrinkage/thresholding algorithm (ISTA)[10], it yields

$$\begin{aligned}\boldsymbol{s}_{i}^{m+1}&=\arg\min_{s_i}\left\{\gamma\left\|\boldsymbol{s}_{i}-\left[\boldsymbol{s}_{i}^{m}-\frac{\nabla f(\boldsymbol{s}_{i}^{m})}{2\gamma}\right]\right\|_{2}^{2}+\|\boldsymbol{s}_{i}\|_{1}\right\}=\\&\arg\min_{s_i}\left\{\gamma\left\|\boldsymbol{s}_{i}-\left[\boldsymbol{s}_{i}^{m}+\frac{-2\alpha\boldsymbol{L}_{ii}\boldsymbol{s}_{i}^{m}-\boldsymbol{h}_{i}+(\boldsymbol{B}^{k})^{\mathrm{T}}\boldsymbol{y}_{i}^{m}}{2\gamma}\right]\right\|_{2}^{2}+\|\boldsymbol{s}_{i}\|_{1}\right\}=\\&\mathrm{shrink}\left(\boldsymbol{s}_{i}^{m}+\frac{-2\alpha\boldsymbol{L}_{ii}\boldsymbol{s}_{i}^{m}-\boldsymbol{h}_{i}^{m}+(\boldsymbol{B}^{k})^{\mathrm{T}}\boldsymbol{y}_{i}^{m}}{2\gamma},\frac{1}{2\gamma}\right)\end{aligned} \tag{14}$$

where $\gamma\geqslant\left[\frac{\lambda\beta}{(2(\lambda+\beta))}\right]\mathrm{eig}((\boldsymbol{B}^{k})^{\mathrm{T}}\boldsymbol{B}^{k})+\alpha\boldsymbol{L}_{ii}$.

2.2.2 $\boldsymbol{B}$-subproblem

We can obtain the rule of updating gradient descent by taking the derivative of Eq. (9) with respect to $\boldsymbol{B}$:

$$\begin{aligned}\boldsymbol{B}^{k+1}&=\boldsymbol{B}^{k}-\zeta[-\boldsymbol{Y}^{k}+\beta(\boldsymbol{B}^{k}\boldsymbol{S}^{k+1}-\boldsymbol{Z}^{k+1})](\boldsymbol{S}^{k+1})^{\mathrm{T}}=\\&\boldsymbol{B}^{k}+\zeta\boldsymbol{Y}^{k+1}(\boldsymbol{S}^{k+1})^{\mathrm{T}}\end{aligned} \tag{15}$$

A normalization of dictionary columns is required after the gradient descent.

2.2.3 $\boldsymbol{u}$-subproblem

In order to achieve faster convergence speed, the variable $\boldsymbol{u}$ is updated at each inner iteration of the Bregman iterative process, which yields

$$\boldsymbol{u}^{k+1}=\arg\min_{u}\left\{\frac{\lambda}{2}\|\boldsymbol{Ru}-\boldsymbol{Z}^{k+1}\|_{\mathrm{F}}^{2}+\frac{\mu}{2}\|\boldsymbol{F}_{\mathrm{p}}\boldsymbol{u}-\boldsymbol{f}^{k}\|_{2}^{2}\right\} \tag{16}$$

The least squares solution satisfies the normal equation,

$$[\mu\boldsymbol{F}_{\mathrm{p}}^{\mathrm{T}}\boldsymbol{F}_{\mathrm{p}}+\lambda\sum_{i}\boldsymbol{R}_{i}^{\mathrm{T}}\boldsymbol{R}_{i}]\boldsymbol{u}^{k+1}=\mu\boldsymbol{F}_{\mathrm{p}}^{\mathrm{T}}\boldsymbol{f}^{k}+\lambda\sum_{i}\boldsymbol{R}_{i}^{\mathrm{T}}z_{i}^{k+1} \tag{17}$$

and yields

$$\boldsymbol{u}(k_x,k_y)=\begin{cases}\boldsymbol{S}_2(k_x,k_y) & (k_x,k_y)\notin\Omega\\ \dfrac{\mu\boldsymbol{f}^{k}(k_x,k_y)+\lambda\boldsymbol{S}_2(k_x,k_y)}{\mu+\omega\lambda} & (k_x,k_y)\in\Omega\end{cases} \tag{18}$$

where $\sum_i\boldsymbol{R}_i^{\mathrm{T}}\boldsymbol{R}_i=\omega\boldsymbol{I}_N$; $\boldsymbol{S}_2=\sum_i\boldsymbol{R}_i^{\mathrm{T}}z_i^{k+1}$; Ω represents the subset of data that has been sampled.

In summary, the proposed Bregmanized method consists of a two-level nested loop. The outer loop updates the variable $\boldsymbol{f}^{k+1}$, while the inner loop alternatively updates the variables $\boldsymbol{B}$, $\boldsymbol{S}$, $\boldsymbol{Z}$, and $\boldsymbol{u}$.

3 Experimental Results

The performance of the TBGSC algorithm is evaluated on several experiments. Its setup is similar to that in Ref. [5], i. e. randomly keeping r pixels in the original image and discarding others. The quality of the reconstruction is quantified using the peak signal-to-noise ratio (PSNR), which is defined as $\mathrm{PSNR}=20\lg\left(\frac{255}{\mathrm{RMSE}}\right)$. Here RMSE is the estimated root mean error between the ground truth and the recovered image. In the first experiment, the comparison was conducted on four images: two edge-dominated and two texture-abundant. Tab. 1 lists the PSNR results of KR, PN and TBGSC methods under different sampling ratios. It can be seen that the proposed TBGSC outperforms all the other methods. In particular, the TBGSC significantly outperforms PN on images with regular texture pattern (e. g., image "Barb2"). This may be because dictionary learning prefers images with highly self-repeating features (as verified in Ref. [12]).

Figs. 1 and 2 show that the TBGSC produces the most visually pleasant results especially for those images with complex texture, indicating better recovery ability under

Tab. 1 PSNR results of three methods under different sampling ratios

r/%	Methods	Lena	Book	Barb2	Barb
25	KR	31.55	31.21	24.64	18.54
	PN	35.45	36.54	29.94	28.26
	TBGSC	35.84	36.69	30.68	28.29
15	KR	29.46	23.76	23.57	17.86
	PN	31.36	31.32	26.06	17.68
	TBGSC	32.10	31.93	28.05	27.01
10	KR	22.27	27.52	22.54	16.61
	PN	29.32	29.26	23.68	16.45
	TBGSC	29.85	29.97	25.14	25.34

higher undersampling ratios. The iterative property of the proposed TBGSC for recovering image "barb2" with r of 15% is illustrated in Figs. 3 and 4. Fig. 3 displays the PSNR value vs. iterations, where the Bregman iteration-based dictionary learning approach demonstrates a notable ability to increase the PSNR value quickly. Fig. 4 depicts the sequence of intermediate recovered image and corresponding dictionaries at the 2nd, 5th, 8th, 15th iterations. It can be observed that from the first to the fifth iterations

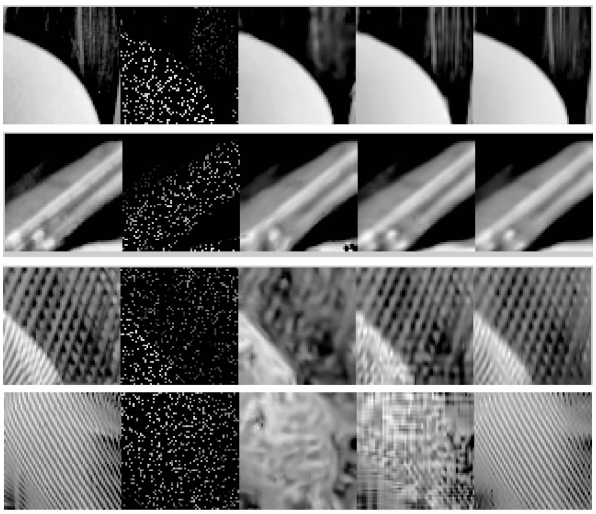

(a) (b) (c) (d) (e)

Fig. 1 Subjective comparison on four toy-example images with r of 15%. (a) Reference image; (b) Observation; (c) KR; (d) PN; (e) TBGSC

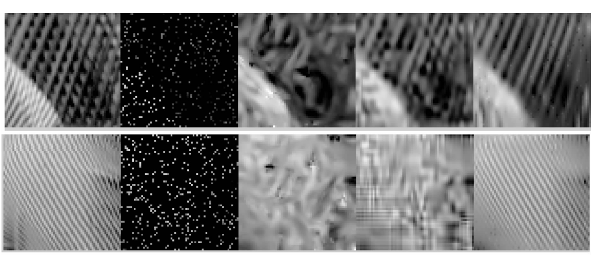

(a) (b) (c) (d) (e)

Fig. 2 Subjective comparison on two toy-example images with r of 10%. (a) Reference image; (b) Observation; (c) KR; (d) PN; (e) TBGSC

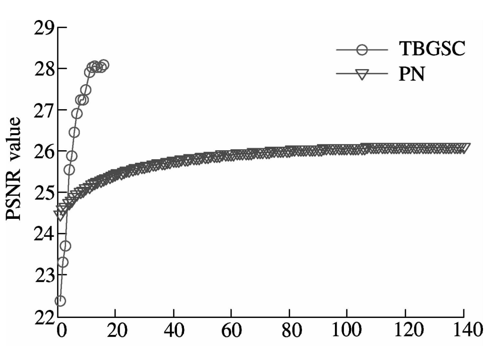

Fig. 3 PSNR value vs. iteration for recovering image "Barb2" by PN and TBGSC with r of 15%

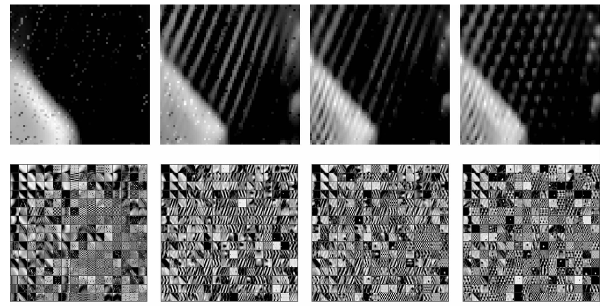

(a) (b) (c) (d)

Fig. 4 Intermediate recovered images (top line) and the corresponding dictionaries (bottom line) generated by TBGSC after iterations with r of 15%. (a) After 2nd iteration; (b) After 5th iteration; (c) After 8th iteration; (d) After 15th iteration

most of the edge objective atoms are constructed and furthermore from the eighth to fifteenth iterations more and more details are added to the atoms. Additionally, the average computation time per iteration is about 4. 19 s. Here, our method was implemented in Matlab 7. 10. 0 on a PC equipped with AMD 2. 31 GHz CPU and 3 GB RAM.

In Fig. 5, the comparison on two generic images "house" and "Lena" is conducted, where $r = 15\%$ is maintained. The recovery PSNR of KR, PN and TBGSC for "house" are 29. 39, 30. 96 and 31. 75 dB, and for "Lena" are 26. 08, 26. 45 and 27. 13 dB, respectively. Fig. 5 shows the enlargements of the reconstruction

(a) (b) (c) (d)

Fig. 5 Subjective comparison on images "house" and "Lena" with r of 15%. (a) Reference image; (b) KR; (c) PN; (d) TBGSC results. Since the proposed method utilizes both the local and nonlocal priors, the image local structure can be better recovered by the TBGSC as observed in Fig. 5. Besides, although PN also aims to exploit the non-local redundancies existing in the image, it may fail and generate some artifacts. It is probably because not many nonlocal redundancies around those structures can be recognized when the observations are highly undersampled. In contrast, our method can overcome this shortcoming by posing the local constraint on the coefficients.

4 Conclusion

In this paper, we propose a two-level Bregmanized method with graph regularized sparse coding for image interpolation. The nonlocal and local geometrical structure information, exploited by graph regularized sparse coding, is incorporated into the two-level Bregmen iterative procedure. Experimental results show that the proposed algorithm outperforms existing algorithms both in terms of vision and PSNR, particularly under highly undersampled observation.

References

[1] Hou H S, Andrews H C. Cubic splines for image interpolation and digital filtering [J]. *IEEE Transactions on Acoustics Speech and Signal Processing*, 1978, **26**(6): 508－517.

[2] Takeda H, Farsiu S, Milanfar P. Kernel regression for image processing and reconstruction [J]. *IEEE Transactions on Image Processing*, 2007, **16**(2): 349－366.

[3] Zhang X J, Wu X L. Image interpolation by adaptive 2-D autoregressive modeling and soft-decision estimation [J]. *IEEE Transactions on Image Processing*, 2008, **17**(6): 887－896.

[4] Liu X M, Zhao D B, Xiong R Q, et al. Image interpolation via regularized local linear regression [J]. *IEEE Transactions on Image Processing*, 2011, **20**(12): 3455－3469.

[5] Li X. Patch-based image interpolation: algorithms and applications [C]//*International Workshop on Local and Non-Local Approximation in Image Processing*. Lausanne, Switzerland, 2008: 1－6.

[6] Dong W S, Zhang L, Lukac R, et al. Sparse representation based image interpolation with non-local autoregressive modeling [J]. *IEEE Transactions on Image Processing*, 2013, **22**(4): 1382－1394.

[7] Zheng M, Bu J J, Chen C, et al. Graph regularized sparse coding for image representation [J]. *IEEE Transactions on Image Processing*, 2011, **20**(5): 1327－1336.

[8] Afonso M, Dias J B, Figueiredo M. An augmented Lagrangian approach to the constrained optimization formulation of imaging inverse problems [J]. *IEEE Transactions on Image Processing*, 2011, **20**(3): 681－695.

[9] Liu Q G, Wang S S, Luo J H, et al. An augmented Lagrangian approach to general dictionary learning for image denoising [J]. *Journal of Visual Communication and Image Representation*, 2012, **23**(5): 753－766.

[10] Yin W T, Osher S, Goldfarb D, et al. Bregman iterative algorithms for l_1-minimization with applications to compressed sensing [J]. *SIAM Journal on Imaging Sciences*, 2008, **1**(1): 142－168.

[11] Xu J, Osher S. Iterative regularization and nonlinear inverse scale space applied to wavelet-based denoising [J]. *IEEE Transactions on Image Processing*, 2007, **16**(2): 534－544.

[12] Dong W S, Li X, Zhang L, et al. Sparsity-based image denoising via dictionary learning and structural clustering [C]//*IEEE Conference on Computer Vision and Pattern Recognition*. Colorado Springs, CO, USA, 2011: 457－464.

基于图结构正则化稀疏表示的双层伯格曼图像插值算法

刘且根[1,2]　张明辉[1]　梁　栋[2]

([1] 南昌大学电子信息工程系，南昌 330031)

([2] 中国科学院深圳先进技术研究院劳特伯生物医学成像研究中心，深圳 518055)

摘要：为了提高图像插值的恢复效果，提出了一种基于图结构正则化稀疏表示的双层伯格曼迭代算法．该迭代算法的外层用于约束图像观测数据，内层用于更新图像块的学习字典和稀疏表示系数．引入的图结构正则化稀疏表示约束可以有效地自适应图像块的局部结构，对于严重受损的情形也能得到精确的恢复结果．此外，在内层迭代中改进的稀疏表示和简洁的字典更新策略使算法能快速地趋于收敛．数值实验结果表明，所提出的算法可以有效地恢复图像，在主观视觉效果和客观量化标准上要优于目前已有的算法．

关键词：图像插值；伯格曼迭代法；图结构正则化稀疏表示；交替方向法

中图分类号：TP391